Toxicology International, *31(4) : 607-620; 2024. DOI: 10.18311/ti/2024/v31i4/44336*

Online ISSN : 0976-5131; Print ISSN : 0971-6580

Toxicology International

Contents available at: www.informaticsjournals.co.in/index.php/toxi



ADMET Assessment, Molecular Docking, and *In Vitro* Antioxidant and Anti-urolithiatic Activities of Natural Furanochrome Khellin

Mounica Ponugoti[1,2], Chakravarthi Guntupalli[1*], Narender Malothu[1] and D. S. N. B. K. Prasanth[3]

[1]KL College of Pharmacy, Koneru Lakshmaiah Education Foundation, Vaddeswaram, Guntur – 522502, Andhra Pradesh, India; chakravarthiguntupalli8@gmail.com

[2]Department of Pharmacology, Hindu College of Pharmacy, Amaravathi Road, Guntur – 522002, Andhra Pradesh, India

[3]School of Pharmacy and Technology Management, SVKM's Narsee Monjee Institute of Management Studies (NMIMS), Polepally SEZ, TSIIC, Jadcherla, Mahbubnagar, Hyderabad – 509301, Telangana, India

Abstract

Urolithiasis is characterized by the formation of urinary calculi and poses a significant health concern due to its associated symptoms and recurrence rates. This study focuses on exploring the phytoconstituents responsible for the anti-urolithic activity of traditionally used *Ammi visnaga* fruits in preventing kidney stones by utilizing various databases and software tools to predict their targets. The small molecules were retrieved from the IMPPAT database and screened for pharmacokinetic attributes, toxicity prediction, and docking analyses using SwissADME, Protox-II, and Autodock Vina. This comprehensive approach identified five key compounds-khellinol, khellin, visamminol, khellol, and visnagin for their drug-like characteristics and interaction potential with target proteins involved in oxidative stress pathways. Further, in vitro assays were conducted to evaluate the antioxidant and anti-urolithiatic activity of khellin, revealing significant IC50 values of 67.39 µg, 36.44 µg, and 134.94 µg for DPPH, hydrogen peroxide scavenging, and superoxide radical scavenging assays, respectively. Additionally, khellin inhibited the oxidation of glutathione by preserving 68.7% of its sulfhydryl groups at a concentration of 200 µg. Concentration-dependent responses were observed in nucleation, aggregation, and growth assays of anti-urolithiatic activity. Notably, khellin demonstrated significant antioxidant effects and inhibition of crystal formation, presenting itself as a potential candidate responsible for preventing urolithiasis. The current study emphasizes the promising role of *Ammi visnaga* fruit phytoconstituents, particularly khellin, as a prospective avenue for managing kidney stone formation, further comprehensive in vivo studies are warranted to validate these outcomes and efficacy under physiological conditions.

Keywords: Antioxidant, Antiurolithiatic Activity, Khellin, Kidney Stones, Molecular Docking

**Author for correspondence*

Article Received on: 04.06.2024 Revised on: 20.08.2024 Accepted on: 22.08.2024

1. Introduction

Urolithiasis is the development of urinary calculi anywhere in the urinary tract including kidneys, ureters, urinary bladder, and urethra[1]. This is primarily due to an imbalance of urinary electrolytes that occurs as a result of dehydration or disparities between the factors that facilitate the crystallization of urine and those that hinder the development and growth of crystals[2]. This is mainly due to the formation of calcium oxalate crystals and their progression into kidney stones was facilitated by membrane impairment. Oxalate-triggered membrane damage was driven by the process of lipid peroxidation, leading to the production of oxygen free radicals as a secondary outcome. Both superoxide anions and hydroxyl radicals were excessively generated in the kidneys causing cellular damage[3].

The most prevalent urinary protein that plays a major role in protection against calcium oxalate crystals is uromodulin. It is synthesized in renal epithelial cells lining the thick ascending limb of the loop of Henle[4]. This protein is involved in renal ion channel regulation, maintenance of salt-water equilibrium, and the modulation of mineral crystallization, all of which are critical processes in kidney stone formation. Altered expression of uromodulin is associated with an increased risk of urolithiasis[5].

Urolithiasis is initially asymptomatic but later it may show symptoms like renal colic, urinary obstruction, frequent and difficulty in urination, urinary tract infection, hematuria, sweating, nausea, and vomiting[6]. Treatment for renal calculi includes extracorporeal shock wave lithotripsy, percutaneous nephrolithotomy, laparoscopic ureterolithotomy, retrograde intrarenal surgery, and drugs such as alpha-blockers, calcium channel blockers, phosphodiesterase – 5 inhibitors (ureteral relaxation); NSAIDs (relieve renal colic); and thiazide and non-thiazide diuretics (prevent recurrence). Even after the use of these many interventional procedures and drug therapies, the relapse was found to be 50% in 5-10 years along with kidney injury[7]. However, the interest in alternative treatments like ancient herbal remedies has increased, offering potential options for kidney stone management. Many plants with secondary metabolites have shown antioxidant and litholytic effects on kidney stones through different mechanisms[8].

In the current study, we examined the phytoconstituents from the traditional medicinal plant *Ammi visnaga,* historically used by Middle Eastern people in the management of kidney stones[9]. Previously, studies were conducted on the fruit extract of *Ammi visnaga* and its compounds against ethylene glycol-induced urolithiasis, revealing that the compounds exhibited a distinct mechanism compared to extract in the management of kidney stones. However, the distinct mechanism was not elucidated[10]. Our current study involved in silico and *in vitro* studies using the phytoconstituents present in *Ammi visnaga* fruit. The phytoconstituents have been screened using Swiss ADMET, molecular docking, and *in vitro* studies. Our findings from the current study have strongly shown that the active phytoconstituent khellin from the plant *Ammi visnaga* exhibits the potential to prevent kidney stones through its antioxidant and anticrystallization properties.

2. Materials and Methods

2.1 Drug Likeness and ADMET Profiling

The phytoconstituents of the plant *Ammi visnaga* fruit have been collected using the largest online database "Indian Medicinal Plants Phytochemistry and Therapeutics" (IMPPAT) (https://cb.imsc.res.in/imppat/home)[11]. Twenty-two phytoconstituents were identified from the above database and their structures (in SDF format) and canonical smiles were retrieved from PubChem database (https://pubchem.ncbi.nlm.nih.gov/). The canonical smiles of the phytoconstituents were submitted to SwissADME (http://www.swissadme.ch/index.php) which enables the computation of physiochemical properties, pharmacokinetics, drug-likeness, and medicinal chemistry[12]. Further, the screened ligands were employed to estimate the organ toxicity, toxicological endpoints, and their LD50 using Pro Tox-II.[13]

2.2 Molecular Docking and Visualization

Molecular docking is the in-silico prediction of ligand-receptor interactions when both molecules are bonded together to generate a stable complex. The 3D structure of ligands was downloaded from PubChem in SDF format. The ligand module of Auto Dock tools liberated all torsional bonds, and gasteiger charges were subsequently calculated and optimized. The RCSB protein data repository was used to extract the PDB files of target proteins catalase (PDB ID:1DGB), superoxide dismutase (PDB ID:4MCM), glutathione-S-transferase (PDB ID:4MPG), and uromodulin (PDB ID: 4WRN) and the active site was identified using the

Computed Atlas of Surface Topography of Proteins (CASTp 3.0) web server[14]. It identifies and characterizes the pockets within the 3D structures of proteins, quantifying their surface area and volume. Additionally, CASTp offers insights into the amino acids contributing to the active site, including their positions. The proteins were prepared by removing water molecules and co-crystalized ligands utilizing BIOVIA Discovery Studio and optimized using Auto Dock tools. Molecular docking was performed using Autodock Vina software to investigate the interactions between ligands and proteins[15]. The algorithm utilized for the docking of proteins incorporates specific configuration parameters which were discussed in the results sections. The interactions are visualized using Discovery Studio Visualizer.

2.3 Chemicals

The chemicals used in the study include khellin, 1,1-diphenyl-2-picrylhydrazyl, nitroblue tetrazolium, phenazine methosulfate, 5,5'-dithiobis-2-nitrobenzoic acid (TCI Chemicals, India), Cystone (Himalaya Herbal Healthcare, India), hydrogen peroxide, EDTA, L-ascorbic acid, calcium chloride, sodium oxalate, sodium chloride, Tris buffer, and sodium acetate (Thermo Fisher Scientific India Pvt Ltd, Mumbai, India).

2.4 *In Vitro* Antioxidant activity

To assess the antioxidant potential of Khellin (KH), we evaluated its ability to scavenge free radicals and inhibit lipid peroxidation.

2.4.1 DPPH Scavenging Activity

For the assessment of free radical scavenging activity, a 0.1 mM solution of 1,1-diphenyl-2-picrylhydrazyl (DPPH) radical in methanol was prepared. Subsequently, 1 ml of this solution was mixed with 3 ml of the KH, Cystone, and L-Asorbic acid (L-AA) at varying concentrations (25, 50, 100, 200 µg). The resulting solutions were incubated for 30 minutes at room temperature, following which the absorbance was measured at 517 nm. A decrease in absorbance of the DPPH solution was indicative of an increase in DPPH radical-scavenging activity. The activity was expressed as the percentage of DPPH radical scavenging and the IC50 value was calculated[16].

2.4.2 Hydrogen Peroxide (H_2O_2) Scavenging Assay

The generation of potential hydroxyl radicals from hydrogen peroxide while undergoing rapid decomposition into oxygen and water, are capable of initiating lipid peroxidation and causing DNA damage in the human body. The capacity of KH to counteract hydrogen peroxide can be assessed by preparing 40 mM hydrogen peroxide in a phosphate buffer (50 mM, pH 7.4). To this various concentrations (25, 50, 100, 200 µg) of KH, Cystone, and L-AA were added and the concentration of hydrogen peroxide was determined by measuring its absorbance at 230 nm using a spectrophotometer after a 10-minute incubation period, with a reference taken from a blank solution that contains phosphate buffer and the percentage of hydrogen peroxide scavenging is calculated[17].

2.4.3 Superoxide Radical Scavenging Assay

In this experimental setup, superoxide radicals were generated within a 3 ml solution of sodium phosphate buffer (100 mM, pH 7.4), which included 1 ml of nitroblue tetrazolium solution (NBT) (150 µM), 1 ml of nicotinamide adenine dinucleotide solution (468 µM), and varying concentrations (25, 50, 100, 200 µg) of KH, Cystone, and L-AA. The reaction was initiated by the addition of 1 ml of phenazine methosulfate solution (60 µM) to the mixture. The reaction mixture was incubated at 25°C for 5 min, and the absorbance was subsequently measured at 560 nm against a corresponding blank solution. As a positive control, L-ascorbic acid was employed. The reduction in NBT, as indicated by changes in absorbance within the reaction mixture, was indicative of KH capacity to scavenge superoxide radicals[18].

2.4.4 Reduced Glutathione Estimation

The following methodology was employed to assess the quantification of sulfhydryl groups of glutathione (GSH) following oxidation induced by H_2O_2. Each sample (varying concentrations of KH, Cystone, and L-AA (25, 50, 100, 200 µg)) was subjected to a 30-minute incubation period at 25°C in a dark environment, utilizing a reaction medium composed of potassium phosphate buffer (1 M, pH 6.8), H_2O_2 (5 mM), and GSH at a concentration of 60 m M. Subsequently, the reaction mixture was combined with 5,5'-dithiobis-(2-nitrobenzoic acid) (DTNB) at a concentration of 10 mM. The absorbance of the resulting solution was measured at 412 nm after a 5-minute interval. Control experiments included samples devoid of GSH serving as blanks, and an incubation medium without the sample was utilized as a control to ensure the accuracy of the measurements[19]. The results were obtained from the formula:

% Remaining sulfhydryls of GSH = [OD of control - (OD of sample – OD of blank)/ OD of control)] x 100

2.5 *In Vitro* Antiurolithiatic activity

2.5.1 Nucleation Assay

The nucleation assay was used to determine the effect of KH on calcium oxalate (CaOx) crystal formation. Calcium chloride and sodium oxalate solutions were prepared at a concentration of 5 mmol/L and 7.5 mmol/L respectively in a buffer containing Tris-Hcl 0.05 mol/L and sodium chloride 0.15 mol/L at 6.5 pH. Various concentrations (25-200 µg/ml) of the test (KH) and standard (Cystone) solutions were prepared in distilled water. Three millilitres of calcium chloride solution were added to each concentration of test and standard followed by the addition of 3 ml of sodium oxalate solution where crystallization starts. The mixture was incubated at 37°C for 30 min. Finally, the optical density (OD) of the solution was estimated spectrophotometrically at 620 nm. The percentage inhibition of nucleation of the test was calculated using the given formula and compared with the percentage inhibition of the standard.

2.5.2 Aggregation Assay

The effect of KH on CaOx crystal aggregation was determined using an aggregation assay. In this assay, the Calcium Oxalate Monohydrate (COM) crystals were prepared by mixing calcium chloride and sodium oxalate at 50 mmol/L each, heated at 60°C for about 1 hour and incubated at 37°C overnight. The CaOx crystals were extracted by centrifugation and were made to a final concentration of 0.8 mg/ml prepared in 0.05 mol/l Tris-Hcl and 0.15 mol/l sodium chloride buffer (pH 6.5). One millilitre of various concentrations of test and standard (25, 50, 100, 200 µg) was added to 3 ml of CaOx solution, mixed, and incubated at 37°C for 30 min. The percentage inhibition of aggregation was evaluated similarly to that of nucleation assay by measuring the OD of the final mixture at 620 nm.

2.5.3 Oxalate Depletion Assay

The oxalate depletion assay was used to assess the effect of KH on the CaOx crystal growth. CaOx stone slurry was prepared in a 50 mM sodium acetate buffer (pH 5.7) at a concentration of 1.5 mg/ml. Each millilitre of 4 mM calcium chloride and 4 mM sodium oxalate was added to 1.5 ml of 10 mM Tris-Hcl and 90 mM sodium chloride buffer (pH 7.4). This was mixed with 30µl of CaOx stone slurry. The oxalate depletion starts after the addition of CaOx slurry, which was measured at 214 nm for 600s to see whether the absorbance disappeared. Subsequently, one millilitre of each concentration of test and standard (25, 50, 100, 200 µg) was added separately to the above solution. The reduction of free oxalate ions was determined by a change in OD and the percentage inhibition of crystal growth was then calculated in the same manner as the nucleation assay[1,20].

2.6 Statistical Analysis

All the experiments were performed in triplicates and were expressed as Mean ± SEM (Standard Error of the Mean). The IC_{50} values were calculated through non-linear regression analysis and the percentage inhibition was determined by applying the formula % Inhibition = [1-(optical density of sample/ optical density of control)] x 100. Statistical analysis was performed on Graph Pad Prism 5 software using ANOVA.

3. Results and Discussion

3.1 Drug Likeness and ADMET Profiling

Following the computer-based assessment of the inhibitory properties of twenty-two phytochemicals derived from *Ammi visnaga,* it was observed that several compounds demonstrated significant potential to exhibit drug-like characteristics. From the pool of phytochemicals, we have identified the most promising candidates that exhibit drug-like characteristics which are presented in Table 1. These compounds include Khellinol, Khellin, Visamminol, Khellol, and Visnagin.

These compounds adhere to a majority of the drug-likeness rules and exhibit favourable ADMET (Absorption, Distribution, Metabolism, Excretion, and Toxicity) properties. Notably, all of these components fully adhere to Lipinski's Rule of Five (RO5), with no violations. Their molar refractivity falls within the range of 40 to 130, their molecular weights are below 500 g/mol, and their log P value falls within the range from -0.7 to 5.0, and the hydrogen bond acceptors are less than 10 and hydrogen bond donors are less than 5, indicating complete adherence to the Ghose filter. The Swiss ADME analysis revealed that all compounds exhibited strong gastrointestinal absorption and can penetrate the Blood-Brain Barrier effectively (except Visamminol

Table 1. Drug-Likeness Predictions using SwissADME for phytochemicals from *Ammi visnaga* fruit

Ligand	Khellinol	Khellin	Visamminol	Khellol	Visnagin
Physicochemical Properties					
Formula	$C_{13}H_{10}O_5$	$C_{14}H_{12}O_5$	$C_{15}H_{16}O_5$	$C_{13}H_{10}O_5$	$C_{13}H_{10}O_4$
Molecular Weight (g/mol)	246.22	260.24	276.28	246.22	230.22
H-bond acceptors	5	5	5	5	4
H-bond donors	1	0	2	1	0
Count					
Rotatable bonds	1	2	1	2	1
TPSA (Å^2)	72.81	61.81	79.9	72.81	52.58
Heavy atoms	18	19	20	18	17
Molar Refractivity	65.74	70.21	74.44	64.88	63.71
Lipophilicity					
XLOGP3	2.49	2.26	2.12	1.04	2.29
Water Solubility					
Silicos-IT Solubility (mg/ml)	8.80E-03	1.86E-03	5.13E-02	8.46E-03	2.18E-03
Silicos-IT class	Moderately soluble	Moderately soluble	Soluble	Moderately soluble	Moderately soluble
Pharmacokinetics					
GI absorption	High	High	High	High	High
BBB permeability	Yes	Yes	No	Yes	Yes
log Kp (cm/s) (Skin Permeation)	-6.03	-6.28	-6.48	-7.06	-6.08
Inhibitor Interaction					
P-gp substrate	No	No	No	No	No
CYP1A2 inhibitor	Yes	Yes	Yes	Yes	Yes
CYP2C19 inhibitor	No	No	No	No	No
CYP2C9 inhibitor	No	Yes	No	No	No
CYP2D6 inhibitor	Yes	No	No	No	No
CYP3A4 inhibitor	Yes	Yes	No	Yes	Yes
Drug-likeness					
Lipinski Rule,	Yes, 0 violations	Yes, 0 violations	Yes, 0 violations	Yes, 0 violations	Yes, 0 violations
Ghose Filter, Veber Rule, Egan Filter, Muegge Filter	Yes, 0 violations	Yes, 0 violations	Yes, 0 violations	Yes, 0 violations	Yes, 0 violations
Bioavailability Score	0.55	0.55	0.55	0.55	0.55
Medicinal Chemistry					
PAINS	0 alert	0 alert	0 alert	0 alert	0 alert
Brenk	0 alert	0 alert	0 alert	0 alert	0 alert
Leadlikeness	1 violation	0 violation	0 violation	1 violation	1 violation
Synthetic Accessibility	2.97	3.16	3.63	2.96	2.89

for BBB permeability). None of these compounds act as substrates for permeability glycoprotein (P-gp). In terms of cytochromes P450 (CYP) interactions, all compounds serve as inhibitors for CYP1A2, and CYP3A4 (except Visamminol). Regarding CYP2C19, none of the compounds demonstrate inhibitory effects. However, for the enzymes CYP2C9 and CYP2D6, all compounds, except for CYP2C9 and khellinol for CYP2D6, do not act as inhibitors.

Further two distinct pattern recognition methodologies PAINS (Pan-assay interference compounds) and Brenk filters were applied. One method, PAINS, identifies molecules that contain specific substructures, irrespective of the protein target, triggering potent responses in assays. Baell et al. identified 481 recurrent fragments, which could lead to false positive outcomes in assays, and Swiss ADME can detect these fragments in the molecule being assessed[21]. Similarly, it integrated structural alert, composed of 105 fragments identified by Brenk et al. as potentially toxic, chemically reactive, metabolically unstable, or associated with poor pharmacokinetics[22]. In our case, there were no alerts detected for PAINS and Brenk criteria across the five compounds.

The absence of toxicity plays a pivotal role in selecting a compound for consideration as a potential therapeutic candidate. In this study, predictions were made regarding organ toxicity specifically hepatotoxicity, and various toxicological endpoints such as carcinogenicity, immunotoxicity, mutagenicity, and cytotoxicity. The results, outlined in Table 2, indicate that all compounds lack hepatotoxicity and cytotoxicity. Khellinol, khellol, and visnagin exhibited carcinogenicity, immunotoxicity, and mutagenicity, khellin demonstrates carcinogenicity and mutagenicity, while visamminol exhibited only mutagenicity. The outcomes of acute toxicity prediction, including LD50 values and toxicity classification on the scale indicated that khellinol, khellin, and khellol belong to Class III and visamminol and visnagin belong to Class IV according to the globally harmonized system of classification of labeling of chemicals.

3.2 Molecular Docking

The Auto Dock Vina algorithm requires various configuration parameters to perform protein docking. These parameters encompass nine binding poses, an exhaustiveness value of 8, and a grid box size set at 30Å x 30Å x 30Å, centred at specific coordinates: Catalase (x = -5.294, y = 25.446, z = 12.933), Superoxide dismutase (x = 37.932, y = 88.791, z = 40.454), Glutathione-S-transferase (x = 12.278, y = 70.466, z = 10.960), Uromodulin (x = 1.215, y = 57.243, z = 31.031). To analyze the diversity in binding affinity scores for individual ligands, multiple docking runs were conducted for each ligand. The selection of the most stable ligand-protein structure relied on identifying the structure with the lowest binding affinity score, hydrogen bonds, and optimal interactions between them (Tables 3-6).

Khellin and visamminol exhibited the lowest binding energies and strong protein-ligand interactions among the compounds studied whereas khellin and khellol displayed a higher number of hydrogen-bond interactions. Specifically, khellol establishes hydrogen bond interactions with amino acid residue A:GLU 330, while visamminol and khellol exhibited hydrophobic interactions with C:HIS 175 resembling L-AA behaviour with catalase. Furthermore, khellinol and khellin exhibited hydrogen bond interactions with adjacent amino acids in superoxide dismutase similar to L-AA. In the case of glutathione-s-transferase, khellinol, khellin, and khellol established hydrogen bonding with the amino acid residue B:GLU 12 whereas visamminol and visnagin interacted with B:ARG 239. Hydrophobic bonds with khellinol, khellin, and khellol and electrostatic interactions with visnagin are observed with the amino

Table 2. Toxicity Prediction of phytochemicals from *Ammi visnaga* fruit computed using Pro-Tox-II

Ligand	LD50 (mg/kg)	Toxicity Class	Organ Toxicity	Toxicity End Points			
			Hepatotoxicity	Carcinogenicity	Immunotoxicity	Mutagenicity	Cytotoxicity
Khellinol	51	3	No	Yes	Yes	Yes	No
Khellin	51	3	No	Yes	No	Yes	No
Visamminol	562	4	No	No	No	Yes	No
Khellol	100	3	No	Yes	Yes	Yes	No
Visnagin	832	4	No	Yes	Yes	Yes	No

Table 3. Molecular docking scores and residual amino acid interactions of phytochemicals from *Ammi visnaga* fruit with Catalase

Ligands	Affinity (Kcal/mol)	Hydrogen Bond Interactions	Hydrophobic Interactions	Electrostatic Interactions
L-Ascorbic acid	-6.7	A:GLU330 (2.58), A:GLU71 (3.08), C:GLU71 (2.94), C:HIS175 (2.24)		
Khellinol	-8.7	A:ARG72 (2.50), A:ARG365 (1.73), A:HIS75 (2.79), A:ARG112 (3.67)	A:HIS75 (4.72), A:HIS75 (5.13)[b], A:TYR358 (5.13)[b], A:VAL146 (4.92)[c], A:HIS75 (3.94)[d], A:TYR358 (4.35)[d], A:TYR358 (4.89)[d], A:ARG72 (4.62)[d], A:ARG112 (4.92)[d], A:ALA133 (4.03)[d], A:ARG72 (5.39)[d], A:ALA133 (5.34)[d]	A: ARG112 (3.80)[e]
Khellin	-8.3	A:ARG72 (1.71), A:ARG365 (2.17), A:ARG365 (2.46), A:ILE332 (3.51), A:HIS362 (3.68)	A: HIS75 (3.70)[a], A:HIS75 (4.76)[b], A:HIS75 (5.28)[b], A:VAL73 (4.63)[c], A:VAL74 (5.03)[c], A:VAL146 (5.07)[c], A:TYR358 (5.18)[d], A:ARG72 (4.75)[d], A:ALA133 (4.57)[d], A:ARG72 (5.05)[d]	A:ARG112 (4.32)[e]
Visamminol	-9	C:ARG170 (2.61), C:GLU119 (2.50)	C:HIS175 (4.68)[g], C:HIS175 (5.15)[g], C:ARG170 (4.91)[c], C:PRO172 (4.85)[c], C:HIS175 (5.27)[d], C:ARG170 (4.47)[d]	A:ARG68 (4.83)[e]
Khellol	-8.1	A:ARG68 (2.73), A:GLU330 (2.18), C:GLU119 (3.65)	C:HIS175 (3.77)[a], C:HIS175 (4.60)[g], C:HIS175 (4.90)[g]	
Visnagin	-8.5	A:ARG72 (2.13), A:ARG365 (2.48)	A:HIS75 (5.16)[b], A:HIS75 (5.43)[b], A:TYR358 (4.47)[b], A:TYR358 (3.94)[b], A:ALA133 (3.93)[c], A:HIS75 (4.81)[d], A:ARG72 (5.23)[d], A:VAL74 (4.88)[d]	

[a]=Pi-Sigma; [b]=Pi-Pi Stacked; [c]=Alkyl; [d]=Pi-Alkyl; [e]=Pi-Cation; [f]=Pi-Anion; [g]=Pi-Pi T-shaped

Table 4. Molecular docking scores and residual amino acid interactions of phytochemicals from *Ammi visnaga* fruit with Superoxide dismutase

Ligands	Affinity (Kcal/mol)	Hydrogen Bond Interactions	Hydrophobic Interactions	Electrostatic Interactions
L-Ascorbic acid	-4.9	J:LYS91 (2.66), F:GLU121 (2.88)		
Khellinol	-5.7	F:LYS122 (3.34)		B:ASP90 (4.89)[f]
Khellin	-5.7	F:LYS122 (3.32)		B:ASP90 (4.87)[f]
Visamminol	-6.7	D:ASN139 (3.34)	D:LYS122 (4.74)[d], D:LYS122 (3.80)[d]	D:LYS122 (4.66)[e]
Khellol	-6.1	B:VAL94 (2.44), B:ASP96 (3.59), F:ASN131 (4.14)		B:ASP90 (4.81)[f]
Visnagin	-5.6	D:ASP125 (3.41), F:GLU40 (3.56)	D:LYS122 (4.18)[c], D:LYS122 (3.74)[d], D:LYS122 (4.55)[d], D:ALA123 (5.15)[d]	D:LYS122 (4.74)[e], D:LYS122 (4.68)[e]

[a]=Pi-Sigma; [b]=Pi-Pi Stacked; [c]=Alkyl; [d]=Pi-Alkyl; [e]=Pi-Cation; [f]=Pi-Anion; [g]=Pi-Pi T-shaped

acid residue B:ARG 239 of glutathione-s-transferase. Khellinol, khellin, khellol and visnagin exhibited hydrogen-bond interactions with the amino acid residue A:GLU 238, resembling the binding pattern observed with the co-crystalized ligand, acetyl glycosamine, in association with uromodulin. Moreover, both khellinol and khellin displayed hydrogen-bond interactions akin to acetyl glucosamine with the amino acid residue A:GLY 37, whereas visamminol demonstrated a hydrophobic bond with uromodulin (Figure 1). Further *in vitro* studies

Table 5. Molecular docking scores and residual amino acid interactions of phytochemicals from *Ammi visnaga* fruit with Glutathione-S-transferase

Ligands	Affinity (Kcal/mol)	Hydrogen Bond Interactions	Hydrophobic Interactions	Electrostatic Interactions
L-Ascorbic acid	-6.3	B:GLN12 (2.40), B:ARG239 (2.34), B:ARG239 (1.90), B:GLY108 (3.45)		
Khellinol	-7.8	B:GLN12 (2.08), B:ARG242 (2.69), B:TRP115 (2.98)	B:TRP115 (3.54)[a], B:TRP115 (5.32)[g], B:TRP115 (5.05)[g], B:TRP115 (4.95)[g], B:TRP115 (5.64)[g], B:LEU35 (4.04)[c], B:LEU114 (4.66)[c], B:TRP115 (4.46)[d], B:TRP115 (5.45)[d], B:ARG239 (4.94)[d], B:ARG239 (5.37)[d]	B:ARG107 (3.54)[e], B:ARG107 (3.55)[e]
Khellin	-7.9	B:GLN12 (2.00), B:ARG242 (2.75), B:TRP115 (2.97)	B:TRP115 (3.57)[a], B:TRP115 (5.35)[g], B:TRP115 (5.68)[g], B:TRP115 (5.05)[g], B:TRP115 (4.98)[g], B:TRP115 (5.64)[g], B:LEU35 (3.96)[c], B:LEU114 (4.62)[c], B:TRP115 (4.53)[d], B:ARG239 (5.01)[d], B:ARG239 (5.42)[d]	B:ARG107 (3.52)[e], B:ARG107 (3.54)[e]
Visamminol	-8.4	B:THR109 (1.78), B:ARG239 (2.35), B:ARG239 (2.17), B:ARG242 (2.72)	B:ARG242 (5.19)[d], B:PRO244 (4.84)[d]	
Khellol	-7.7	B:GLN12 (2.03), B:GLN12 (2.41), B:ARG242 (2.78), B:GLY111 (3.31), B:GLY111 (3.46), B:ARG239 (4.15), B:TRP115 (2.82), B:ARG239 (2.52)	B:TRP115 (5.06)[g], B:TRP115 (4.83)[g], B:TRP115 (5.21)[g], B:TRP115 (4.83)[g], B:LEU35 (5.40)[d], B:ARG239 (5.45)[d]	B:ARG107 (3.38)[e], B:ARG107 (3.97)[e], B:ARG239 (4.37)[e], B:ARG239 (4.15)[e]
Visnagin	-7.7	B:ARG239 (2.11), B:GLY111 (3.27), B:ARG239 (4.12), B:TRP115 (3.22), B:TRP115 (2.69)	B:TRP115 (5.33)[g], B:TRP115 (5.29)[g], B:TRP115 (4.79)[g], B:TRP115 (5.05)[g], B:TRP115 (5.33)[g], B:LEU35 (4.03)[c], B:HIS40 (4.49)[d], B:LEU35 (5.23)[d]	B:ARG107 (3.68)[e], B:ARG107 (3.90)[e], B:ARG239 (4.12)[e]

[a]=Pi-Sigma; [b]=Pi-Pi Stacked; [c]=Alkyl; [d]=Pi-Alkyl; [e]=Pi-Cation; [f]=Pi-Anion; [g]=Pi-Pi T-shaped

are planned based on the above ADMET and molecular docking studies focusing on khellin.

3.3 *In Vitro* Antioxidant Assays

3.3.1 DPPH Scavenging Activity

The capacity of khellin to scavenge DPPH radicals, thereby transforming the stable purple DPPH radical into its non-radical yellow form was assessed across different concentrations. Figure 2(A) illustrates the reduction of DPPH radical activity in a dose-dependent manner after the introduction of various concentrations of khellin (25-200 µg/ml). At a concentration of 200 micrograms, the inhibition of free radicals by L-AA, Cystone, and, khellin was recorded as 89.37±0.162%, 72.94±0.364%, and 85.19±0.202%, respectively. The calculated IC50 values for Cystone and khellin were 54.28 µg and 44.78 µg, respectively, in comparison to 41.43 µg for L-AA.

3.3.2 Hydrogen Peroxide Scavenging Assay

Figure 2(B) showcases a comprehensive overview of hydroxy radical scavenging activity exhibited by Cystone and khellin at various concentrations in comparison to L-AA. The activity of each compound was observed to increase as the concentration rose, with khellin exhibiting greater inhibition than L-AA at a concentration of 50 and 100 µg without any significant difference. Notably, at the highest concentration, Cystone and khellin showed a percentage inhibition of 82.38±0.452 and 87.530±1.20 respectively compared to L-AA (92.47±0.352). The IC50 values were found to be 49.92 µg, 59.36 µg, and 46.55 µg respectively for L-AA, Cystone, and, khellin.

Table 6. Molecular docking scores and residual amino acid interactions of phytochemicals from *Ammi visnaga* fruit with Uromodulin

Ligands	Affinity (Kcal/mol)	Hydrogen Bond Interactions	Hydrophobic Interactions	Electrostatic Interactions
Acetyl glucosamine	-6.4	A:ASN258 (2.14), B:ARG465 (2.64), B:ARG465 (2.67), B:SER462 (2.67), A:GLU238 (2.20), A:GLY37 (3.61)		
Khellinol	-7.3	B:GLY490 (2.76), A:GLU238 (3.44), A:GLY37 (3.46),	A:GLY37 (3.75) [h], A:ASP38 (4.15) [h], B:VAL492 (5.04) [c]	
Khellin	-7.3	B:GLY490 (2.76), A:GLU238 (3.45), A:GLY37 (3.48),	A:GLY37 (3.72) [h], A:ASP38 (4.10) [h], B:VAL492 (5.13) [c], A:TYR41 (5.03) [d], A:HIS63 (4.91) [d], A:TYR234 (4.00) [d]	
Visamminol	-8.1	B:ASP463 (2.83), B:GLY487 (3.66)	A:GLY37 (4.68) [h], A:ASP38 (3.89) [h], B:VAL492 (4.93) [c]	
Khellol	-7.0	B:THR491 (2.30), B:SER462 (3.43), A:GLU238 (3.73)		B:ASP463 (4.54) [f]
Visnagin	-7.0	B:SER462 (3.45), A:GLU238 (3.65)	B:VAL492 (4.84) [c]	B:ASP463 (4.54) [f]

[a]=Pi-Sigma; [b]=Pi-Pi Stacked; [c]=Alkyl; [d]=Pi-Alkyl; [e]=Pi-Cation; [f]=Pi-Anion; [g]=Pi-Pi T-shaped; [h]= Amide-Pi Stacked

3.3.3 Superoxide Radical Scavenging Assay

Superoxide free radicals and the activated intermediates they produce are known to play a role in causing tissue damage during oxidative stress. Khellin and Cystone demonstrated notable inhibition of superoxide radicals in a manner dependent on dosage as depicted in Figure 2(C). At a concentration of 200 µg, Cystone and khellin displayed notable difference ($p<0.001$) scavenging activities of 56.13±0.393% and 67.03±0.416%, respectively, which were lower than that of the standard compound L-AA 73.62±0.421%. The observed IC50 values of the compounds were 58.59 µg, 113.6 µg, and 126.0 µg of L-AA, Cystone, and khellin respectively.

3.3.4 Reduced Glutathione Estimation

The effect of khellin on the percentage of remaining sulfhydryl groups of glutathione has shown effects similar to L-AA with no significant difference, as shown in Figure 2(D). Nonetheless, all the tested treatments demonstrated the ability to inhibit the oxidation of GSH. This was evidenced by the preserved sulfhydryl groups of GSH that were still able to react with DTNB after the oxidation process was induced by the addition of hydrogen peroxide. Notably, at the highest concentration (200 µg) tested, L-AA, Cystone, and khellin inhibited the oxidation of glutathione, thereby protecting the sulfhydryls at a percentage of 73.2, 64.6, and 68.7, respectively.

3.4 *In Vitro* Antiurolithiatic Activity

Urolithiasis is the result of a series of processes that begin with the nucleation of crystals, growth, aggregation, and retainment in the kidneys. CaOx urinary stones are the most common type of urinary stones. Calcium oxalate monohydrate is the predominant component of calcium oxalate stones and its prevalence is roughly double that of Calcium Oxalate Dihydrate (COD)[23].

3.4.1 Nucleation Assay

The pathophysiology of CaOx urolithiasis begins with nucleation. Nucleation is a thermodynamically induced phase transition in which dissolved components in a supersaturated solution precipitate abruptly, which will be observed in nucleation assay. Consequently, urolithiasis could be minimized if nucleation of crystals or subsequent phases in crystallization is inhibited. As a result, this characteristic of the test compound is beneficial in reducing urinary stone formation by promoting the expulsion of tiny particles from the kidney and lowering the risk of retention in the urinary tract.

The control group (Figure 3A) exhibited several hexagonal and rectangular COM crystals with pointed edges. Khellin (Figure 3F-I) at lower concentrations and Cystone (Figure 3B-E) at higher concentrations promoted the development of tetrahedral and tetragonal COD crystals with smoother architecture. These

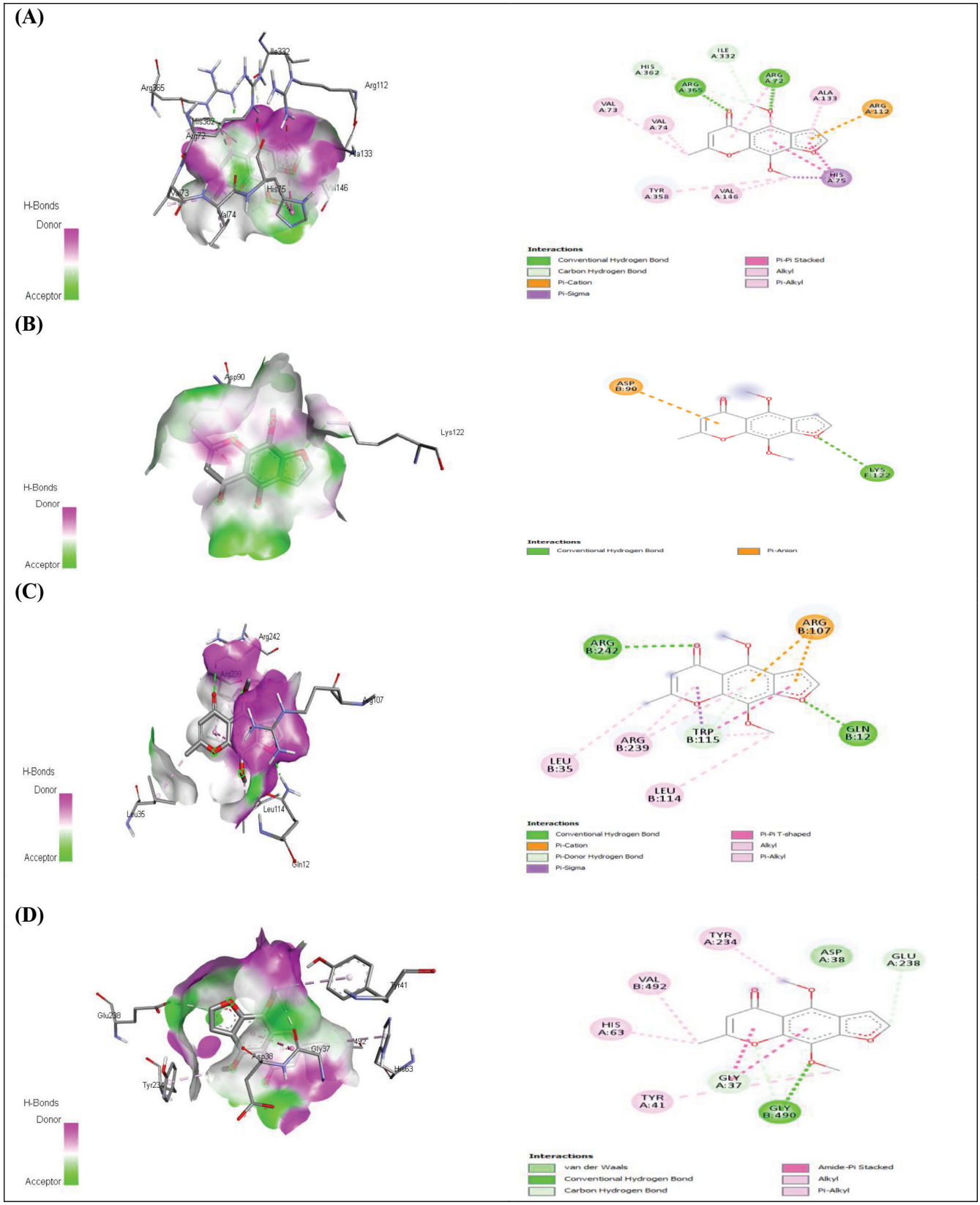


Figure 1. 3D and 2D view depicting the binding interactions of Khellin with **(A)** Catalase, **(B)** Superoxide dismutase, **(C)** Glutathione-S-transferase, and **(D)** Uromodulin.

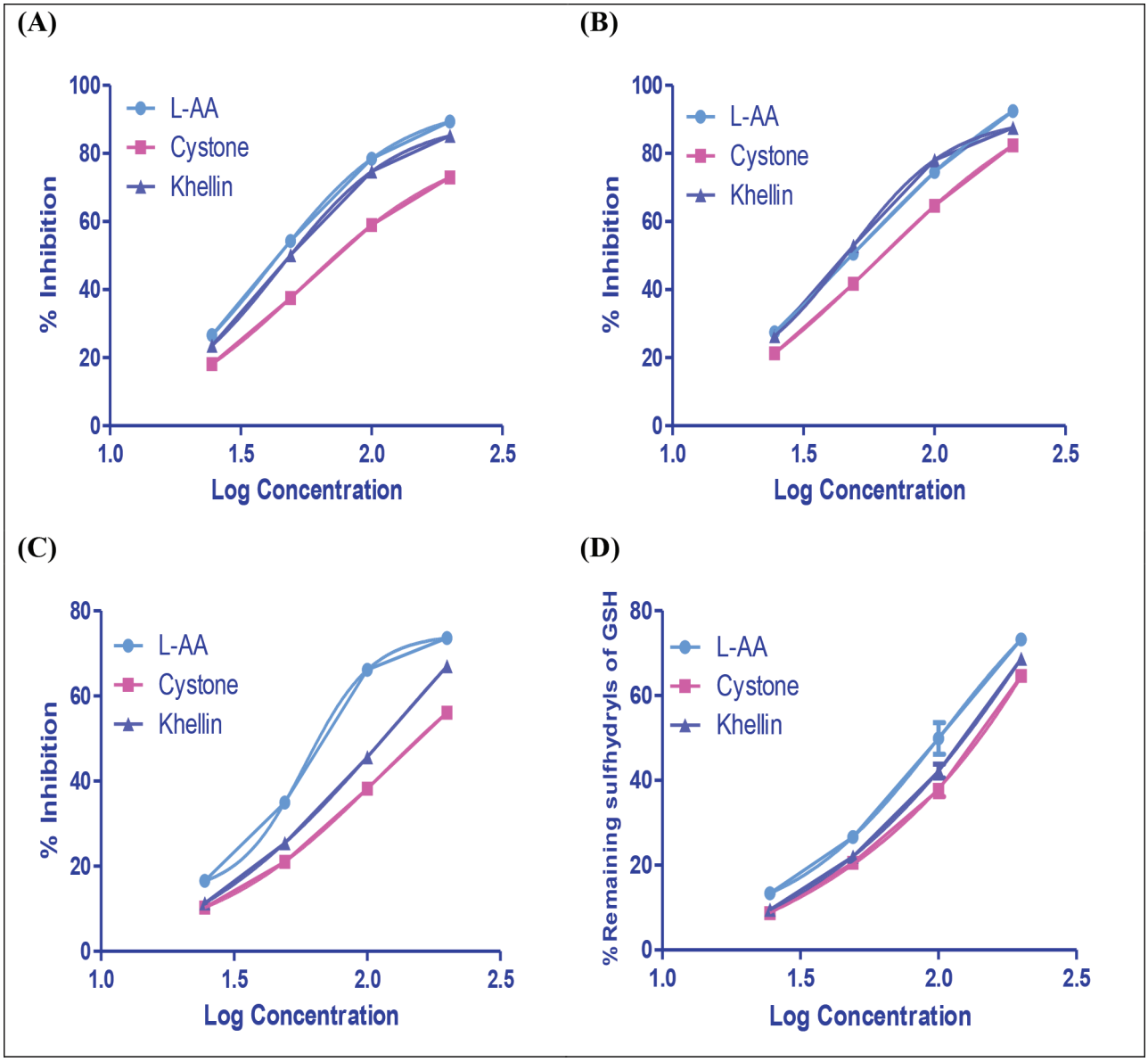


Figure 2. Illustrates the free radical scavenging activity of Cystone and Khellin on **(A)** DPPH radicals, **(B)** Hydroxy radicals, **(C)** Superoxide radicals, and **(D)** % Remaining sulfhydryls of glutathione. L-AA was used as the standard antioxidant for comparison and performed in triplicates.

crystals are readily eliminated in the urine compared to COM and minimize the development of kidney stones. With increasing concentrations, Khellin hindered crystallization by preventing CaOx nucleation by dissolving into tiny particles. In the presence of the test compound, there was a significant reduction in the CaOx crystal nucleation when compared to Cystone. This signifies that the test compound has anti-crystallization properties in CaOx nucleation assay. KH (91.2±017) significantly ($p<0.001$) inhibited nucleation compared to compared to Cystone (89.01±18) at 200 µg/ml.

3.4.2 Aggregation Assay

CaOx crystals nucleate, grow, and begin to interact and merge to form aggregates which retained in the kidney. Of the two crystalline forms, COM crystals are more stable than COD crystals with a higher tendency to aggregate. COD has a low adhesion property compared to COM. Hence, the adhesion and aggregation tendency of COM leads to the retainment of these crystals in the kidney leading to renal cell injury. Whereas COD with its lowest adhesion property evacuated in urine[24]. The morphology

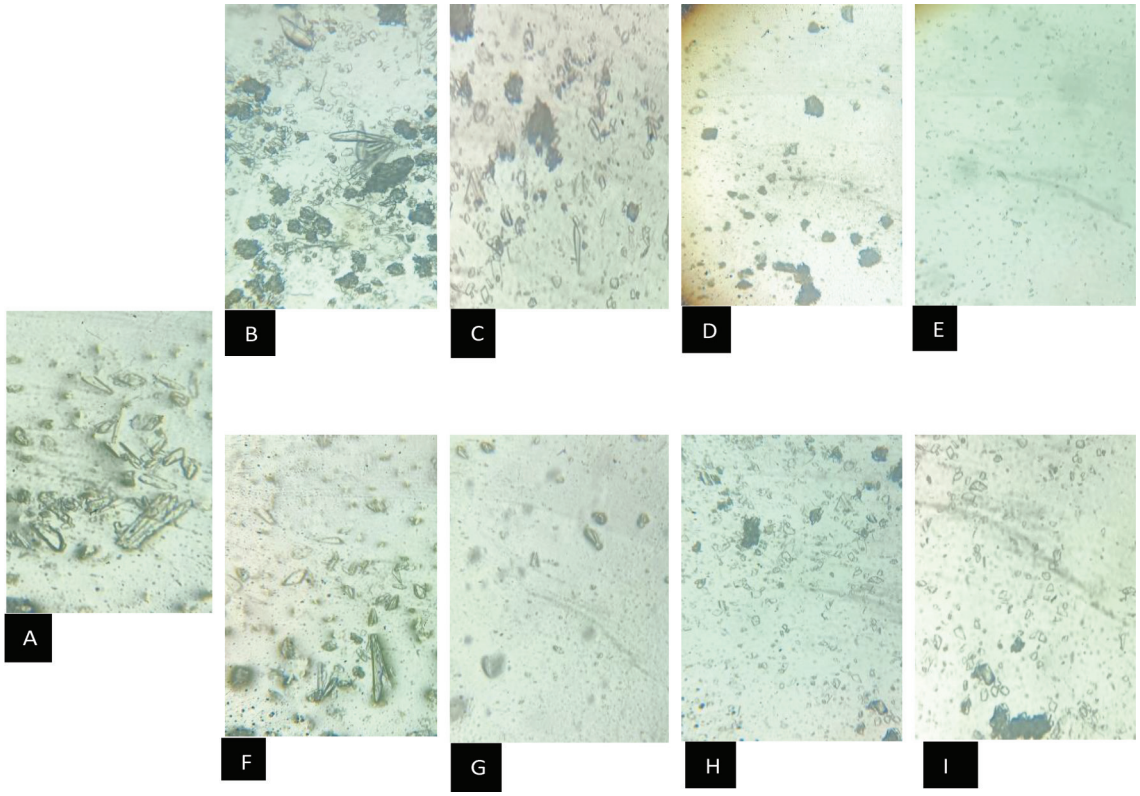


Figure 3. Photomicrographs of CaOx crystals as observed under a light microscope (40x) in the absence A, and in the presence of Cystone 25 µg/ml B, 50 µg/ml C, 100 µg/ml D, 200 µg/ml E, and Khellin 25 µg/ml F, 50 µg/ml G, 100 µg/ml H, 200 µg/ml I.

of COM crystals was altered by KH in the microscopic investigation.

Crystal aggregation is the process through which a large number of crystals join together and bind to form massive crystal agglomerates. These aggregates retain in renal tubular cells favoring stone formation[25]. KH and Cystone inhibited the aggregation of CaOx crystals 82.85±0.45, 80.32±0.11 respectively at a concentration of 200 µg/ml (Figure 4).

3.4.3 Oxalate Depletion Assay

The adsorption of crystal-forming ions on the CaOx crystal lattice in the supersaturated solution results in CaOx crystal growth by reducing the overall free energy. Hence, crystal growth is one of the important criteria for the development of kidney stones. The percentage reduction of free oxalate by KH was found to be significant (64.79±0.16) ($p<0.001$) compared to Cystone (59.71±0.32) at a concentration of 200µg/ml (Figure 4). The test compound significantly reduced the growth of CaOx crystals when compared to the positive control Cystone. Hence these compounds may contain nucleation-inhibiting elements that hinder the CaOx crystal growth.

Khellin (a natural furanochrome) has exhibited *in vitro* antiurolithiac activity through different mechanisms. Our investigation revealed substantial antioxidant activities of khellin across various assays, including its ability to scavenge DPPH, hydroxyl, and superoxide radicals. These findings are in agreement with Vanachayangkul *et al.*, 2010[10] which suggested that reducing the production of radical oxygen species might prevent renal tubular epithelial cell injury caused by oxalate and calcium oxalate monohydrate crystals.

Glutathione, a vital intracellular antioxidant, plays a pivotal role in protecting cells against oxidative damage[26]. L-Ascorbic acid, used as a standard in the present study, can directly reduce oxidized glutathione (GSSG) back to its reduced form (GSH) by donating electrons to GSSG. This process is crucial for maintaining intracellular GSH levels, especially during oxidative stress conditions[27]. Notably, khellin inhibited the oxidation of glutathione by protecting its sulfhydryl groups which further supports its antioxidant role. khellin's ability to enhance glutathione

levels suggests its potential to bolster the antioxidant defense system. A study on khellin also revealed its ability to modulate nitric oxide synthase thereby decreasing oxidative stress[28].

Under normal physiological conditions, uromodulin inhibits the growth and aggregation of COM crystals. However, when uromodulin becomes saturated with calcium, it loses its ability to inhibit crystal growth, aggregation, and crystal-cell adhesion. Extensive genetic and *in vivo* evidence strongly support uromodulin's role as a potent inhibitor in kidney stone formation. Despite some conflicting studies, further clarification is needed regarding the exact mechanism and the specific stage of crystal formation affected by uromodulin[29].

In this study, khellin transformed rectangular COM crystals into spherical COD crystals by decreasing their diameter, potentially aiding in the prevention of kidney stone formation. However, further *in vivo* studies are essential to substantiate these findings, since many contributing factors strongly impact the formation and attachment of kidney stones, causing damage to renal epithelial cells.

4. Conclusion

The damage to renal epithelial cell membranes caused by crystal nucleation, accumulation, growth, and elevated oxalate concentrations results in lipid and protein peroxidation, leading to CaOx crystal adhesion and subsequent development into kidney stones. The current investigation revealed the in silico and *in vitro* efficacy of khellin in scavenging free radicals and inhibiting CaOx crystallization. Furthermore, the formation of complexes with calcium and oxalate which inhibits the nucleation process, conversion, and reduction of pointed-edged COM to blunt COD crystals, aggregation, and crystal growth, indicates its litholytic activity. In light of these findings, khellin, an active phytoconstituent of *Ammi visnaga*, might be responsible for its anti-urolithiatic activity. The various stages in kidney stone formation are regulated by the equilibrium between stone promoters and inhibitors, the pH of the urine, the amount of water excreted, and the concentration of the stone-forming elements *in vivo*. However, our observations were conducted solely in silico and *in vitro*. Therefore, further comprehensive long-term *in vivo* studies are imperative to validate khellin's efficacy under these physiological conditions robustly.

5. Acknowledgements

The authors would like to thank the authorities of KL University and Hindu College of Pharmacy for providing the necessary facilities for the successful completion of research work.

6. References

1. Sasikala V, Radha SR, Vijayakumari B. *In vitro* evaluation of Rotula aquatica Lour. for antiurolithiatic activity. J Pharm Res. 2013; 6(3):378-82. https://doi.org/10.1016/J.JOPR.2013.02.026
2. Heilberg IP, Schor N. Renal stone disease: causes, evaluation and medical treatment. Arq Bras Endocrinol Metab. 2006; 50(4):823-31. https://doi.org/10.1590/S0004-27302006000400027
3. Selvam R. Calcium oxalate stone disease: role of lipid peroxidation and antioxidants. Urol Res. 2002; 30(1):35-47. https://doi.org/10.1007/s00240-001-0228-z
4. Schaeffer C, Devuyst O, Rampoldi L. Uromodulin: Roles in health and disease. Annu Rev Physiol. 2021; 83:477-501. https://doi.org/10.1146/annurev-physiol-031620-092817
5. Micanovic R, LaFavers K, Garimella PS, Wu XR, El-Achkar TM. Uromodulin (Tamm–Horsfall protein): Guardian of urinary and systemic homeostasis. Nephrol Dial Transplant. 2019; 35(1):33-43. https://doi.org/10.1093/ndt/gfy394
6. Alelign T, Petros B. Kidney stone disease: an update on current concepts. Adv Urol. 2018; 2018:1-12. https://doi.org/10.1155/2018/3068365
7. Shafi H, Moazzami B, Pourghasem M. An overview of treatment options for urinary stones. Caspian J Intern Med. 2016; 7(1):1-6. https://doi.org/10.22088/cjim.7.1.1
8. El Menyiy N, Khouchlaa A, El Omari N, Zengin G, Gallo M, Montesano D, *et al.* Litholytic activities of natural bioactive compounds and their mechanism insights. Appl Sci. 2021; 11(18):8702. https://doi.org/10.3390/app11188702
9. Khalil N, Bishr M, Desouky S, Salama O. *Ammi visnaga* L., a potential medicinal plant: A review. Molecules. 2020; 25(2):301. https://doi.org/10.3390/molecules25020301
10. Vanachayangkul P, Byer K, Khan S, Butterweck V. An aqueous extract of *Ammi visnaga* fruits and its constituents khellin and visnagin prevent cell damage caused by oxalate in renal epithelial cells. Phytomedicine. 2010 Jul;17(8-9):653–8. https://doi.org/10.1016/j.phymed.2009.10.011
11. Mohanraj K, Karthikeyan BS, Vivek-Ananth RP, Chand RPB, Aparna SR, Mangalapandi P, *et al.* IMPPAT: A curated database of Indian medicinal plants. Sci Rep. 2018; 8(1):4329. https://doi.org/10.1038/s41598-018-22631-z
12. Daina A, Michielin O, Zoete V. SwissADME: A free web tool to evaluate pharmacokinetics, drug-likeness and

medicinal chemistry friendliness of small molecules. Sci Rep. 2017; 7(1). https://doi.org/10.1038/srep42717
13. Banerjee P, Eckert AO, Schrey AK, Preissner R. ProTox-II: A webserver for the prediction of toxicity of chemicals. Nucleic Acids Res. 2018; 46(W1):W257-63. https://doi.org/10.1093/nar/gky318
14. Tian W, Chen C, Lei X, Zhao J, Liang J. CASTp 3.0: Computed atlas of surface topography of proteins. Nucleic Acids Res. 2018; 46(W1):W363-7. https://doi.org/10.1093/nar/gky473
15. Trott O, Olson AJ. AutoDock Vina: Improving the speed and accuracy of docking with a new scoring function, efficient optimization, and multithreading. J Comput Chem. 2009; 31(2):455-61. https://doi.org/10.1002/jcc.21334
16. Eruygur N, Koçyiğit UM, Taslimi P, Ataş M, Tekin M, Gülçin İ. Screening the *in vitro* antioxidant, antimicrobial, anticholinesterase, antidiabetic activities of endemic *Achillea cucullata* (Asteraceae) ethanol extract. South Afr J Bot. 2019; 120:141-5. https://doi.org/10.1016/j.sajb.2018.04.001
17. Ruch RJ, Cheng S, Klaunig JE. Prevention of cytotoxicity and inhibition of intercellular communication by antioxidant catechins isolated from Chinese green tea. Carcinogenesis. 1989; 10(6):1003-8. https://doi.org/10.1093/carcin/10.6.1003
18. Robak J, Gryglewski RJ. Flavonoids are scavengers of superoxide anions. Biochem Pharmacol. 1988; 37(5):837-41. https://doi.org/10.1016/0006-2952(88)90169-4
19. Sachett A, Gallas-Lopes M, Conterato GMM, Herrmann AP, Piato A. Antioxidant activity by reduced Glutathione (GSH) assay: *In vitro* protocol v1. 2021. https://doi.org/10.17504/protocols.io.btaynifw
20. Bawari S, Sah A N, Tewari D. Antiurolithiatic activity of *Daucus carota*: An *in vitro* study. Pharmacogn J. 2018; 10(5):880-4. https://doi.org/10.5530/pj.2018.5.148
21. Baell JB. Feeling nature's PAINS: Natural products, natural product drugs, and Pan Assay Interference compounds (PAINS). J Nat Prod. 2016; 79(3):616-28. https://doi.org/10.1021/acs.jnatprod.5b00947
22. Brenk R, Schipani A, James D, Krasowski A, Gilbert I, Frearson J, *et al*. Lessons learnt from assembling screening libraries for drug discovery for neglected diseases. Chem Med Chem. 2008; 3(3):435-44. https://doi.org/10.1002/cmdc.200700139
23. Sun XY, Xu M, Ouyang JM. Effect of crystal shape and aggregation of calcium oxalate monohydrate on cellular toxicity in renal epithelial cells. ACS Omega. 2017; 2(9):6039-52. https://doi.org/10.1021/acsomega.7b00510
24. Wesson JA, Ward MD. Role of crystal surface adhesion in kidney stone disease. Curr Opin Nephrol Hypertens. 2006; 15(4):386-93. https://doi.org/10.1097/01.mnh.0000232879.50716.6f
25. Chaiyarit S, Thongboonkerd V. Defining and systematic analyses of aggregation indices to evaluate degree of calcium oxalate crystal aggregation. Front Chem. 2017; 5. https://doi.org/10.3389/fchem.2017.00113
26. Yan F, Yang W, Li X, Lin T, Lun Y, Lin F, *et al*. A trifunctional enzyme with glutathione S-transferase, glutathione peroxidase and superoxide dismutase activity. Biochim Biophys Acta Gen Subj. 2008; 1780(6):869-72. https://doi.org/10.1016/j.bbagen.2008.03.003
27. Biswas P, Dellanoce C, Vezzoli A, Mrakic-Sposta S, Malnati M, Beretta A, *et al*. Antioxidant activity with increased endogenous levels of vitamin C, E and A following dietary supplementation with a combination of glutathione and resveratrol precursors. Nutrients. 2020; 12(11):3224. https://doi.org/10.3390/2072-6643/12/11/3224
28. Guntupalli C, Ponugoti M, Prasanth DSBK, Malothu N. Cerebroprotective effects of khellin: Validation through computational studies in a bilateral common carotid artery occlusion/reperfusion (BCCAO/R) model. Mol Simul. 2024; 50(4):322-31. https://doi.org/10.1080/08927022.2024.2307530
29. Thielemans R, Speeckaert R, Delrue C, De Bruyne S, Oyaert M, Speeckaert MM. Unveiling the hidden power of uromodulin: A promising potential biomarker for kidney diseases. Diagnostics. 2023; 13(19):3077. https://doi.org/10.3390/diagnostics13193077